

## Hard Si-C-N Chemical Vapor Deposited Films

O.K. Porada<sup>1</sup>, A.O. Kozak<sup>1</sup>, V.I. Ivashchenko<sup>1</sup>, S.M. Dub<sup>2</sup>, A.D. Pogrebnyak<sup>3</sup>

<sup>1</sup> Institute for Problems of Materials Sciences, NAS of Ukraine, 3, Krzhynanovskyy Str., 03142 Kyiv, Ukraine

<sup>2</sup> Institute for Superhard materials, NAS of Ukraine, 2, Avtozavodskaya Str., 03142 Kyiv, Ukraine

<sup>3</sup> Sumy State University, 2 Rymysky-Korsakov Str. 40007 Sumy, Ukraine

(Received 30 June 2015; published online 29 August 2015)

Si-C-N thin films were deposited on silicon substrates by plasma-enhanced chemical vapor deposition (PECVD) using hexamethyldisilazane as the main precursor. An influence of substrate temperature ( $T_s$ ) on film properties was analyzed. It was established that the deposited films were x-ray amorphous. The growth of the films slows down with increasing substrate temperature. The distribution of Si-C, Si-N and C-N bonds were almost independent of  $T_s$ , whereas the number of C-H, Si-H and N-H bonds essentially decreased when substrate temperature increased. The nanohardness and elastic modulus increased with  $T_s$  due to a reduction of the weak hydrogen bonds.

**Keywords:** Si-C-N films, PECVD, hexamethyldisilazane, substrate temperature, nanohardness.

PACS numbers: 81.15.Gh, 73.61.Jc, 62.20.Qp

### 1. INTRODUCTION

The investigation of Si-C-N films shows that nanohardness ( $H$ ) can change from 6 to 40 GPa depending on deposition procedure [1-7]. Amorphous hydrogenated Si-C-N films that are deposited using photo-CVD (Photo-chemical vapor deposition), PECVD (Plasma-enhanced chemical vapor deposition), ECR-CVD (Electron cyclotron resonance - chemical vapor deposition) [1,3] demonstrate the lowest values of nanohardness 6-11 GPa [2,4,5]. The highest values of nanohardness are reached for the films prepared by high-temperatures (more than 1000 °C) CVD (Chemical Vapor Deposition) (27-38 GPa) [1,3] and PVD (Physical Vapor Deposition) (25-40 GPa) [8]. The films usually have the amorphous structure, while the nanocrystalline or polycrystalline films are prepared at extreme deposition parameters (for example, at high deposition temperatures > 1000 °C). In the literature, the values of nanohardness ( $H$ ) and elastic modulus ( $E$ ) of the Si-C-N films are often reported in the range of 18-25 GPa and 110-200 GPa, respectively [2-7]. The influence of the main parameters of PECVD on the structural and mechanical properties of Si-C-N films was studied by us earlier. In particular, the influence of discharge power [9], nitrogen flow rate [10], substrate bias voltage [11], substrate temperature [12] and vacuum annealing [13] on film characteristics were analyzed. The maximum values of nanohardness and elastic modulus were 25 GPa and 200 GPa, respectively [9-12].

In this work we continue the investigation of Si-C-N films to reach larger values of the hardness of the Si-C-N films preserving their amorphous structure. The latter is very important, because amorphous films are more resistant to oxidation than nanocrystalline ones. We increased substrate temperature to 700 °C as compared to the maximum  $T_s = 400$  °C used in Ref. [12]. The deposited films were characterized by X-Ray diffraction, FTIR spectroscopy and nanoindentation.

### 2. EXPERIMENTAL DETAILS

Si-C-N thin films were deposited with using high-frequency plasma-chemical equipment on base of "VUP-5" (Ukraine). The main discharge was excited by high-frequency (HF) generator (40.68MHz). Hexamethyldisilazane (HMDS,  $(\text{CH}_3)_6\text{Si}_2\text{NHN}$ ) was used as a main precursor. The HMDS vapor, produced in a thermostated bubbler heated to 40 °C, was transported into the reaction chamber by hydrogen. Substrate bias was produced by a HF generator (5.27 MHz). The films were deposited on polished Si(001) substrates.

The films were deposited at different substrate temperatures  $T_s = 300, 400, 500, 650$  and  $700^\circ\text{C}$  and at fixed other deposition parameters: substrate bias - 250 V, gas mixture pressure in the reactor 0.2 Torr, discharge power  $P_w = 0.2 \text{ W/cm}^2$ , flow rate of hydrogen through the thermostated bubbler with HMDS  $F_{\text{H+HMDS}} = 12 \text{ sccm}$ , nitrogen flow rate  $F_{\text{N}_2} = 1 \text{ sccm}$ . Deposition time was 60 min.

X-ray diffraction (XRD) investigations of the films were carried out by using a diffractometer "DRON-3M" (Ukraine). The chemical bonding was studied by Fourier transform infrared spectroscopy (FTIR) with the help of a spectrometer "FSM 1202" LLC "Infraspek". Nanoindentation was carried out with the help of a device G200 equipped with the Berkovich indenter. Nanohardness ( $H$ ) and elastic modulus ( $E$ ) were determined using the Oliver and Pharr procedure [14]. The thickness of the films was estimated by an optical profilometer "Micron - alpha" (Ukraine). The film thickness approximated 0.8  $\mu\text{m}$ , and slightly decreased with increasing  $T_s$ .

### 3. RESULTS AND DISCUSSION

The XRD analysis showed that there are no any crystallites in the deposited films (not shown here). It follows that they are X-Ray amorphous.

Fig. 1 shows the substrate temperature influence on the deposition rate of Si-C-N films. The increase of  $T_s$  up to 400°C leads to noticeable increase in deposition rate,

which can be connected with additional thermal stimulation of chemical reactions on the surface of the substrate. A further increase of  $T_s$  leads to decreasing deposition rate due to the predominance of the densification process due to hydrogen effusion from films and sputtering the weakly bonded units from the film surface.

In Fig. 2 we present the dependences of nanohardness and elastic modulus of the films deposited at different  $T_s$  as functions of indenter penetration ( $L$ ). It is clearly seen that the elastic modulus is more sensitive to substrate than nanohardness:  $E$  reaches the maximum values at the indentation depth  $\sim 25$  nm, and then decreases with further increasing  $L$ .

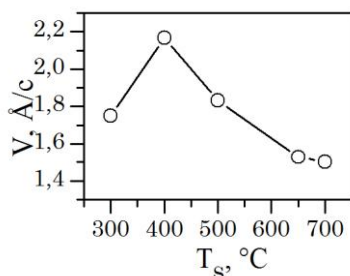


**Fig. 1** – Dependence of Si-C-N film deposition rate ( $V$ ) on substrate temperature ( $T_s$ ).

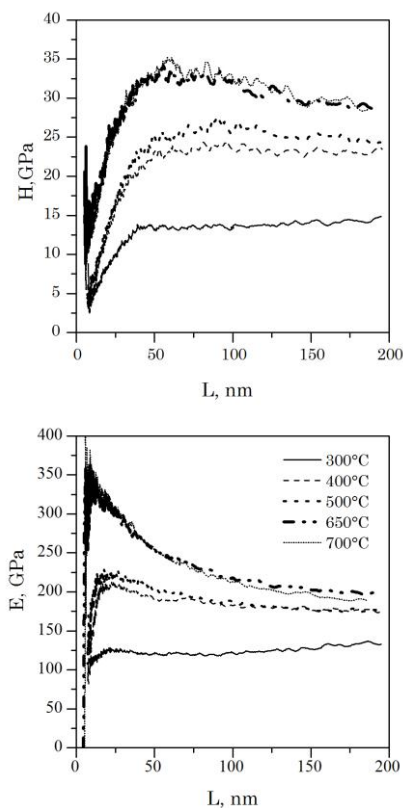


**Fig. 2** – Nanohardness ( $H$ ) and elastic modulus ( $E$ ) as functions of indenter penetration ( $L$ ).

In Fig. 3 we show the value of  $H$  and  $E$  of the deposited films as functions of  $T_s$ . These values were determined as the maximum values in the dependences shown in Fig. 2. From Fig. 3 it is clearly seen that  $H$  and  $E$  increases with  $T_s$ .

The analysis of the properties of Si-C-N films [9-13] shows that the mechanical characteristics are very sensitive to substrate temperature. On the other hand, the mechanical properties depend on the chemical bonding. In this work, we investigate the character of chemical bonding of the deposited films using the FTIR spectroscopy.

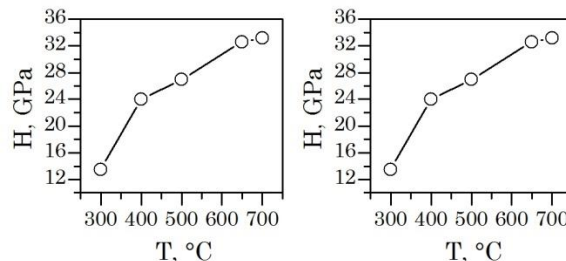


**Fig. 3** – Nanohardness ( $H$ ) and elastic modulus ( $E$ ) as functions of substrate temperature ( $T_s$ ).

The FTIR absorption spectra of the Si-C-N films deposited at various substrate temperatures are presented in Fig 4a. The absorption bands were identified on the basis of published data [17-24]. In the FTIR spectra, the dominant absorption broad band in the range of 600–1300  $\text{cm}^{-1}$  and four absorption bands in the range 1300–3500  $\text{cm}^{-1}$  are observed. The preliminary analysis shows that the dominant absorption band can be interpreted as vibrations of Si-C (610–877  $\text{cm}^{-1}$ ) [24], Si-N (950–1000  $\text{cm}^{-1}$ ) [23] and Si-O (1000–1030  $\text{cm}^{-1}$ ) [18] bonds. Absorption bands in the range of 1300–3500  $\text{cm}^{-1}$  can be attributed to vibrations of C-C bonds at 1555  $\text{cm}^{-1}$ , C-N [18] and/or Si-H [20] bonds at 2130  $\text{cm}^{-1}$ , as well as vibrations of hydrogen bonds C-H [21] and N-H [19,20] at 2877  $\text{cm}^{-1}$  and 3375  $\text{cm}^{-1}$ , respectively. It is easy to see that the intensity of hydrogen bonds in the range of 1550-3500  $\text{cm}^{-1}$  gradually decreases with increasing substrate temperature, while the change in the main absorption band at 600-1300  $\text{cm}^{-1}$  is barely visible. In order to analyze the contributions of different vibrations to this band and their evolution with substrate temperature we present the main absorption band as a superposition of three Gaussians. Fig. 4b shows the results of decomposition of the FTIR spectra in the range of the main absorption band into Gaussian components. The chosen area is represented by three components, and, for ease of perception, it is inversed relatively to the horizontal axis. Given the band identifications [10], the Gaussian components can be assigned to vibrations of Si-C [24], Si-N in  $\text{Si}_3\text{N}_4$  [16] and Si-O [25] bonds (cf. Fig 4b). The total area of the Gaussian peaks is practically independent of substrate temperature. It is seen that Si-C bonds are predominant. Also, besides the mentioned vibrations, the following vibrations related to hydrogen bonds can contribute to the main absorption band: vibrations of  $(\text{SiH}_2)_n$  bonds with peak at 915  $\text{cm}^{-1}$ , Si-H bonds at 978  $\text{cm}^{-1}$  and  $\alpha$ -SiC-H and C-H<sub>n</sub> bonds at 990  $\text{cm}^{-1}$  [16]. Unfortunately, the analysis of hydrogen bonds within the main absorption band is practically impossible owing to the presence of the intensive vibrations of Si-C, Si-N and Si-O bonds in this absorption region. Nevertheless, we can assume that the reduction of Gaussian peak at 975  $\text{cm}^{-1}$  with increasing of substrate

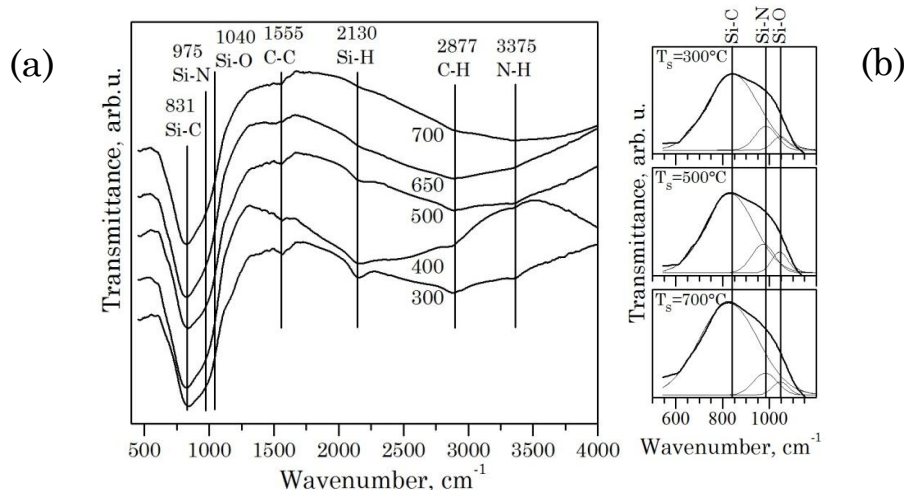


**Fig. 4** – FTIR absorption spectra of the films deposited at different substrate temperatures  $T_s = 300\text{--}700$  °C (a). Results of the decomposition of the main absorption band by three Gaussian components (b).

temperature is due to hydrogen effusion. We note a tendency to reducing the intensity of the vibrations of hydrogen bonds at 2130, 2877 and 3375  $\text{cm}^{-1}$  with increasing  $T_s$ . In our PECVD technologies, hydrogen is a plasma gas, and therefore its content is very high in the films deposited at low  $T_s$ . A moderate substrate temperature (less than 500 °C) leads to formation of hydrogenated structure of the Si-C-N films that is characterized by the presence of Si-H, C-H and N-H bonds. The hydrogenated structure promotes the formation of the pores that leads to decreasing film density, and to the deterioration of mechanical properties. So, the films deposited at low  $T_s$  will exhibit low hardness due to the hydrogenated porous structure. At higher substrate temperatures, the formation of hydrogen bonds slows down, which leads to the formation of the denser structures, and in turn, to strengthening of the films.

## REFERENCES

1. A. Bendeddouche, R. Berjoane, et al., *J. Appl. Phys.* **81**, 6147 (1997).
2. Y. Awad, M.A. El et al., *Surf. Coat. Technol.* **204**, 539 (2009).
3. A. Bendeddouche, R. Berjoan, et al., *Surf. Coat. Technol.* **111**, 184 (1999).
4. Z. Shi, Y. Wang et al., *Appl. Surf. Sci.* **259**, 1328 (2011).
5. Z. Shi, Y. Wang et al., *J. Alloy. Compnd.* **552**, 111 (2013).
6. S. Peter, M. Günther, et al. *Vacuum* **90**, 155 (2013).
7. H.C. Lo, J.J. Wu, et al., *Diam. Rel. Mater.* **10**, 1916 (2001).
8. J. Vlček, M. Kormunda, et al., *Surf. Coat. Tech.* **160**, 74 (2002).
9. L.A. Ivaschenko, V.I. Ivaschenko, et al., *Nanostructured Materials Science* **4**, 42 (2011) [in Ukrainian].
10. V.I. Ivashchenko, A.O. Kozak et al., *Thin Solid Films* **569**, 57 (2014).
11. O.K. Porada, *Nanostructured Materials Science* **3-4** 32, (2014) [in Ukrainian].
12. A.O. Kozak, V.I. Ivashchenko, et al., *J. Nano- Electron. Phys.* **6**, 04047(2014).
13. O.K. Porada, V.I. Ivashchenko, *Nanostructured Materials Science*, **2**, 32 (2010) [in Ukrainian].
14. W.C. Oliver, G.M. Pharr, *J. Mater. Res.* **7**, 1564 (1992).
15. I. Maissel, R. Glang, *Handbook of Thin Film Technology* (In 2v.- New York: McGRAW HILL HODK COMPAN **2**, 765, 1970).
16. Y. Awad, M.A. El Khahani, et al., *J. Appl. Phys.* **107**, 033517 (2010).
17. A. Bendeddouche, R. Berjoan, et al., *Surf. Coat. Technol.* **111**, 184 (1999).
18. J. Huran, A. Valovič, et al., *J. Electr. Eng.* **63**, 333 (2012).
19. D. Kuo, D. Yang, *Thin Solid Films* **374**, 92 (2000).
20. Z. Shi, Y. Wang et al., *Appl. Surf. Sci.* **258**, 1328 (2011).
21. B.P. Swain, N.M. Hwang, *Appl. Surf. Sci.* **254**, 5319 (2008).
22. X.-C. Xiao, Ya-W. Li, et al., *Appl. Surf. Sci.* **156**, 155 (2000).
23. M. Xu, S. Xu, et al., *J. Non-Cryst. Solids* **352**, 5463 (2006).
24. X.B. Yan, B. Tay, et al., *Electrochem. Comm.* **8**, 737 (2006).
25. X.C. Wu, R.Q. Cai, et al., *Appl. Surf. Sci.* **185**, 262 (2002).